200 kW / 500 kW Solar-electric Modular Flexible Kinetic Escort (SMo-FlaKE)

Department of Aerospace Engineering, A. James Clark School of Engineering,
University of Maryland, College Park
Advisor: David Akin

Team Sol Invictus

Ryan Ernandis
Leandre Jones
Hermann Kaptui
Shaheer Khan
Rounak Mukhopadhyay

Abstract

As advances in electric propulsion and solar power continue, the idea of using solar electric propulsion for orbit maneuvering is gaining significance interest. This paper proposes the construction of a Solar Electric Propulsion (SEP) tug which will ferry payloads from LEO to LDRO. The Solar-electric Modular Flexible Kinetic Escort (SMo-FlaKE) is designed to be launched in multiple parts and assembled in space. It will operate at 200 kW and is expandable to up to 500 kW.

SECTION 1: Configuration

The SMo-FlaKE is designed to be as modular as possible. Initially, the SMo-FlaKE will consist of 2 engine modules and 1 central payload-bearing module. The central payload-bearing module has docking stations for up to 4 total engine modules and 1 docking station for the payload. It also contains the robotic arm named Yeti and the small fine arm named Ermine. The engine modules each contain 2 NASA-457m Hall Effect thrusters, Xenon propellant tanks, radiators, and have 2 solar panels attached to them, as well as the required plumbing, wiring, and avionics required to operate the thrusters.

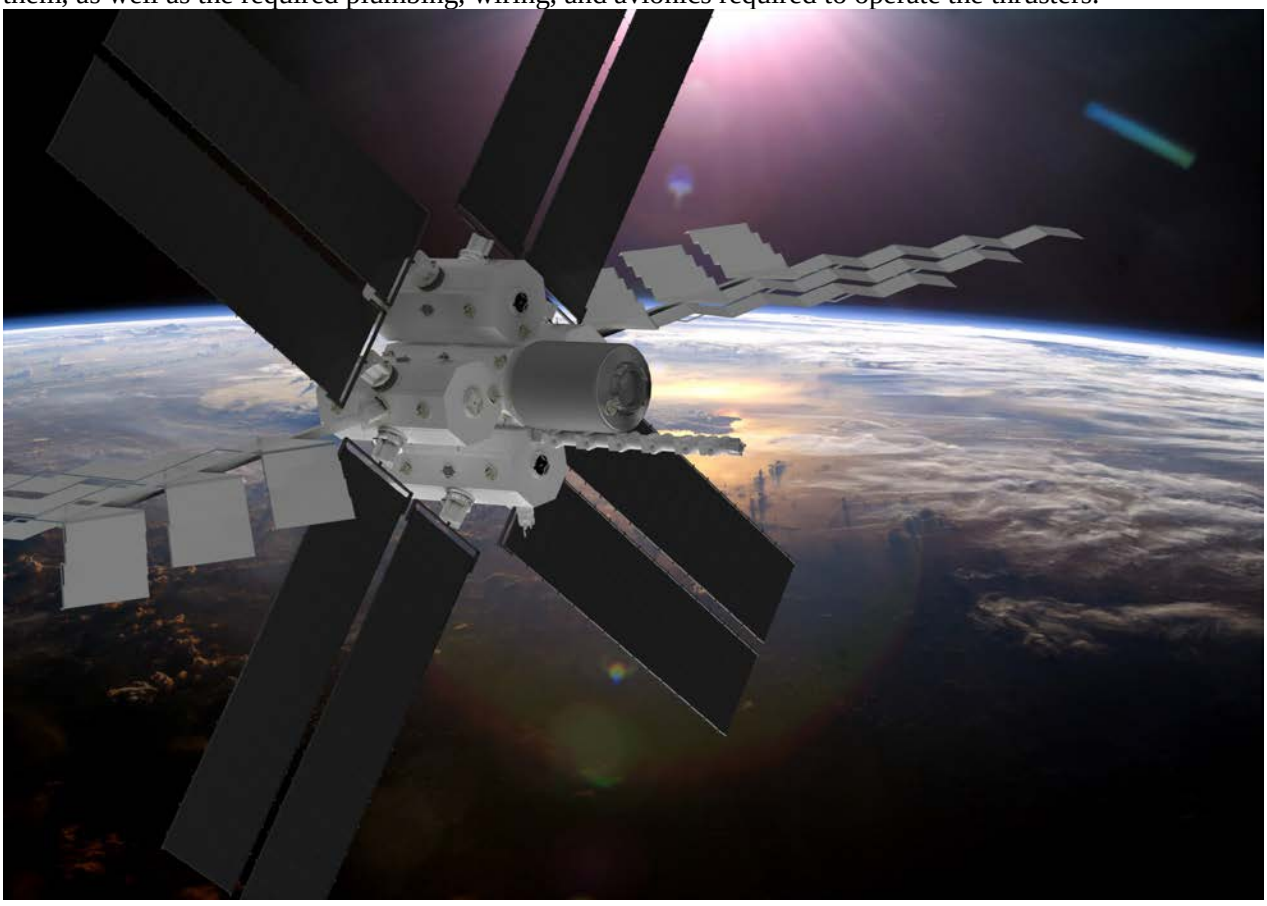

Figure 1.1 Full spacecraft configuration

SECTION 2: Docking, Berthing, and Inter Module Connections

Autonomous assembly requires robust sensors capable of relaying all the information required for an autonomous control scheme, therefore a docking sensor trade study was conducted between the NFAVGS and TriDAR systems.

The NFAVGS sensor (23) relays basic information of range and includes a large spotting range of 2 km and a 15-30 m docking range. With a tiny power consumption for 35 watts, this sensor accomplishes its requirements. However, the autonomous assembly and docking of SMo-FlaKE requires an intensive control scheme and additional sensor information.

TriDAR uses a combination of triangulation, LIDAR 3D imaging, and thermal imaging for autonomous rendezvous and docking. The 3D Model Based Tracking works up to about 3 km, and a full 6 Degree of Freedom (DOF) pose can be generated up to 200 km. TriDAR is immune to lighting conditions and requires no cooperative targets. The sensor system uses a 3D model of the target as a reference and all processing is performed locally on the sensor (20). We decided to use TriDAR over the NFAVGS because of its superior range and additional benefits.

The outer modules will be connected to the center module using a variant of the Common Berthing Mechanism (CBM) found on the International Space Station (ISS). The center module will be launched with active CBM rings, and each outer module will be launched with a passive CBM ring. When the outer modules are delivered to the spacecraft, each outer module will align itself with the center module using the TriDAR sensors. Once aligned the passive CBM ring will be captured by the latches and the bolting procedure will take place. The CBM connection will have to withstand 0.4 g's of acceleration, which is 268,000 N of force for the 500kW configuration. Taking into account any payload that may be attached, we found the highest payload mass would be from the Delta IV Heavy which can hold up to 278,000 N, which gives the connection an additional 111,000 N (25). Assuming each bolt will be able to hold 85,900 N, each CBM connection would require 5 bolts (14).

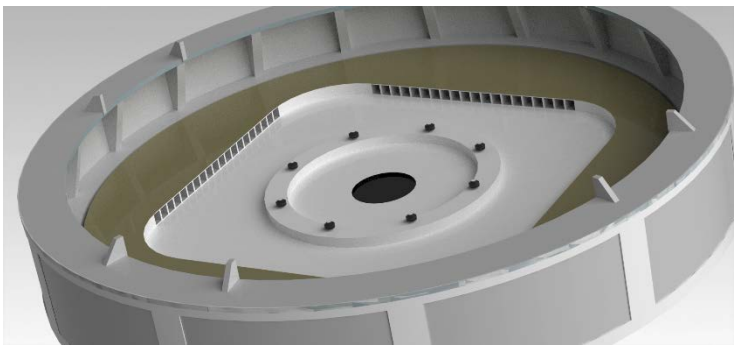

Figure 2.1: Male quick connects on 28-1 Series valve uses a dry-break quick disconnect

Once the modules are successfully bolted together fluid and power lines will be attached to the active and passive CBM rings and replace the section normally used for the crew hatch. There will be 2 power lines and 8 fluid lines across each CBM. The power lines will be fed into the three batteries in the center module which will be used to power Yeti and the grapple fixtures. We decided on two power lines in case of failure of one, we would still be able to charge the central module batteries with the second power line. The fluid lines will be transporting the Xenon, RCS Fuel and Oxidizer, and Ammonia; each fluid will have its respective inflow and outflow pipes. After the outer module has successfully berthed with the center module the fluid and power lines will extend from the outer module using a gear mechanism with a small motor. The power lines will use simple pronged connections and the fluid lines will use quick connects to attach from the passive CBM to the active CBM. The 8 male quick connects on the passive CBM ring can be seen in Figure 2.1.

The quick connects must be able to withstand the pressures within the fluid systems. We modeled the thermal control system after that found on the ISS, and found that the radiator system has a nominal pressure of 300 psi or 20.7 bar, and a maximum pressure of 500 psi, or 34.5 bar (1). The 200N Bipropellant RCS Thruster has an inlet pressure range of 13 - 24 bar, or 188.5 psi - 348.1 psi (1). Using these specifications we decided on modeling our quick connect after the Parker Snap-tite 28-1 Series which has a maximum working pressure of 1000 psi. The safety factor for system pressure will thus be 2 for the maximum radiator pressure case. The 28-1 Series valve uses a dry-break quick disconnect which minimizes the amount of lost fluid during disconnect and maintains worker safety when ground testing the fluid systems (18).

The CBM rings will be integrated into the modules during construction and therefore will not be able to be repaired independently of its respective module. Any minor misalignments of the power and

fluid lines will be resolved by Yeti, but if a CBM ring stops functioning properly then the entire module will have to be replaced.

SECTION 3: Solar Panels

The process of choosing the solar panels started with gathering information on a range of solar panels and cells. Using the information found, the area required to produce both 200 kW and 500 kW was calculated based on the efficiency using where the power required was 200 kW and the insolation constant is 1394 W/m^2. Using this information we chose the solar panels requiring the lowest area, as shown in Figure 3.1. The area per array was also calculated using four solar arrays.

Solar Array:	Cell Type	Efficiency:	Power Density (W/m^2):	Area for 200 kW (m^2):	Area for 500 kW (m^2):	Area per Array 200 kW (m^2):	Area per Array 500 kW (m^2):
AEC-Able Ultraflex Silicon	Silicon	0.17	115	844	2110	211	527
AEC-Able Ultraflex GaAs	Gallium Arsenide	0.23	140	624	1559	156	390
NASA CEV-Orion (now MPCV)	Triple Junction (TJ)	0.28	390	512	1281	128	320
Orbital ATK Cygnus	ZTJ Luna	0.29	404	495	1237	124	309
SolAero ZTJ Space Solar Cell	3rd Gen ZTJ	0.30	411	486	1216	122	304
Spectrolab NeXt Triple Junction	XTJ GaInP2/GaAs/Ge	0.31	428	467	1168	117	292

Figure 3.1: Initial Solar Array Calculations (16,24)

From the calculations in Figure 3.1, the Spectrolab NeXt Triple Junction solar arrays were chosen as they provided the highest power density and smallest area needed per array in both the 200 kW and 500 kW cases. Using the information provided by Spectrolab shown in Figure 3.2, data showing the specifications for panels was used to calculate more precise area measurements and mass calculations based on both beginning of life (BOL) and end of life (EOL) cases. Panel areas of greater than 2.5 m^2 were chosen as the solar panels would be large and a 3 mil ceria doped coverslide was also chosen as it provided a lighter mass for the solar panels.

Spectrolab XTJ					
Premade panels:	**BOL Power (W/m^2):**	**EOL Power (W/m^2):**	**Design Decisions:**		
Panel Area >2.5 [m^2]:	366	351.36		**BOL**	**EOL**
Panel Area <2.5 [m^2]:	345	331.2	Length (m):	28	28
Mass:	**(kg/m^2):**		Width (m):	5	5
3 mil Ceria Doped Coverslide	1.76		# of Panels:	4	4
6 mil Ceria Doped Coverslide	2.06		Area of Panels (m^2):	140	140

	Area (m^2):				
Area needed for 200kW:	546.45		Power Per Panel (kW):	51.24	49.19
Area per panel for 4 arrays:	136.61		Total Power (kW):	204.96	196.76
			Additional Solar Panels		
			Length (m):	30	30
			Width (m):	7	7
			# of Panels:	4	4
			Area of Panels (m^2):	210	210
			Power Per Panel (kW):	76.86	73.79
			Total Power (kW):	512	491

Figure 3.2: Spectrolab XTJ Solar Arrays (24)

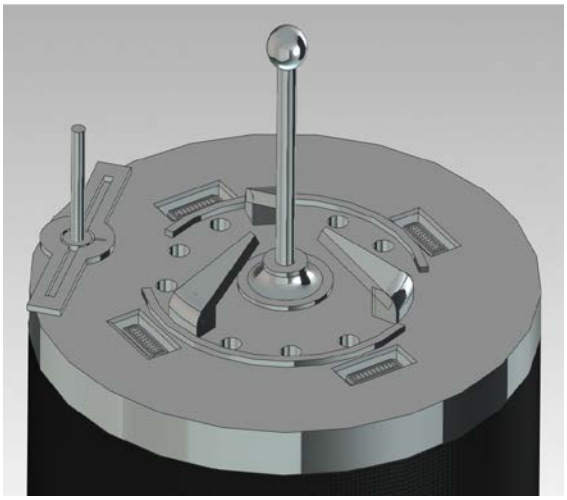

Figure 3.3 Solar Panel Probe

Figure 3.4 Solar Panel Alpha Joint

As shown in Figure 3.2, we calculated that we will start with 4 solar arrays of area 140 m^2 which will provide 205 kW at BOL and 197 kW at EOL. For the spacecraft to expand to 500 kW, we have calculated that we will need to add 4 solar panels of area 210 m^2 which will provide an additional 307 kW at BOL and 295 kW at EOL. With the addition of the extra solar arrays, the total power produced by the solar arrays would be 512 kW at BOL and 492 kW at EOL.

The retractable solar panels are initially launched in their folded configuration. They will individually be enclosed in canisters and flown detached from the other parts of the spacecraft. Once delivered near the outer modules, Yeti will attach them to the external modules. Due to the energy requirement of design, every outer module will be equipped with two solar-panels deployment systems (oriented at 90° apart). They will be attached to the central module using a probe/drogue mechanism inspired from the hybrid SSVP-M8000, which is currently used on the ISS. The probe (fig. 3.4) will consist of an extended probe equipped with a soft capture latch. The probe will ensure captured before contact, during the berthing phase. The female interface will consist of a soft latch capture. The Yeti will be used to rotate the encapsulated solar panel in the correct position. A pattern of claws will be used for alignment purposes. The hard latch located at along the rim of the docking mechanism will lock the two interfaces together. After the connection is established, the solar panels will deploy using a scissor lift mechanism attached to the module. Once deployed, the electric current will flow from the panels to the batteries through the electric connection integrated inside the docking system. The orientation of the solar panels will be monitored by a tracking sensor, and an Alpha joint, shown in figure 3.4, will allow for a smooth rotation of the panels.

SECTION 4: Power Distribution

All power from the solar arrays goes through the power distribution system. SMo-FlaKE's power distribution system revolves around a yet to be built direct-drive unit (DDU) capable of handling the 50

kW needed to power and control the NASA-457MV2 50 kW Hall Thruster engines rather than a power processing unit capable of the same specifications. The reason for choosing the DDU over the PPU is the mass savings. We calculated that the PPU would weigh 92 kg. The calculated DDU mass is 19 kg.

This DDU will be used in conjunction with each engine individually, processing the power provided by the solar panels. The DDUs will also allocate the power from the solar panels to the batteries stored in each module of the spacecraft. The DDUs will be connected together to evenly distribute all power generated to the electronics equipment located throughout the vehicle. A few of the main electronics required onboard would be the sun sensor which would be used to locate the sun and relay the information to the solar array joints and drivers. The power will also be made to power the communications equipment in the spacecraft.

SECTION 5: Batteries

When searching for the batteries we made sure to confirm the options could operate in space and were Lithium-Ion. We decided on Lithium-Ion because they last twice as long as Nickel-Hydrogen and have smaller cell sizes (9). The search brought us to Saft Batteries, a company dedicated to creating advanced-technology batteries for many different industries. We looked at the space-qualified Saft catalog included in Figure 5.1 and optimizing for specific energy and volume we decided on the VL51ES battery cell. Saft offers to manufacture batteries with 12 cells in parallel per battery, which will give a total capacity of 2.2 kW-h per VL51ES battery. Each NASA-457MV2 50 kW Hall Thruster engine will draw 50 kW with 2 engines on each of our outer modules. The total power draw from our engines will be 200 kW. The center module will draw 10 kW, 3 kW will go to Yeti and Ermine and the additional 7 kW is allotted for charging capabilities for the payload. The spacecraft will be solely drawing from the batteries only when in darkness, which was calculated to be a maximum of 37 minutes in the closest orbit. The total power needed while in darkness will be 130 kW-h. With each battery providing 2.2 kW-h, we will need 28 batteries for each engine module and 3 batteries for the center module. In order to avoid fully discharging the batteries, we decided to double the capacity and include 56 batteries in each engine module and 6 batteries in the center module. With this analysis for the 200 kW spacecraft, we will need 118 VL51ES batteries to run all three modules. After expanding to 500 kW, the 2 additional outer modules will result in a total of 230 VL51ES batteries.

	VES 140	VES 180	VL 48E	VL51ES	VES 16	VL 6P
Guaranteed capacity (Ah)	39	50	48	51	4.5	6.6
Mean voltage at C/1.5	3.6	3.6	3.6	3.6	3.6	3.6
End of charge voltage (V)	4.1	4.1	4.1	4.1	4.1	4.1
Energy (Wh)	140	180	170	180	16	22
Specific energy (Wh/kg)	126	165	150	170	155	65
Height (mm)	250	250	250	222	60	143
Diameter (mm)	53	53	54	54	33	38.2
Weight (kg)	1.13	1.11	1.13	1.08	0.155	0.34
Power capability current pulses A						225
Main application	GEO, MEO	GEO, MEO	GEO, LEO	GEO, MEO,LEO	LEO,GEO	Launcher

Figure 5.1: Saft's Li-ion cell catalog (20)

SECTION 6: Propulsion

In order to select an adequate propulsion system, the following assumptions were made. Firstly, the SEP tug was launched into low Earth orbit at an altitude of 167 km. Secondly, the tug's acceleration is completely in the tangential direction. Now, the proportional delta-V for low thrust can be calculated by the vis-viva equation. From LEO to LDRO, the delta-V was calculated to be approximately 7.1 km/s. Afterward, the engine selection process begun by researching various design reference missions and specifications sheets of electric propulsion systems. During this process, six electric propulsion engines were selected for further consideration. The considered engines are tabulated below in Figure 6.1.

	VASIMR	NEXT	NASA-457MV2 50 kW Hall Thruster	Busek BHT-20 kW Hall Thruster	NSTAR Ion Engine	300MS 20 kW Hall Thruster
Acceleration (m/s^2)	1.67E-04	1.42E-07	1.53E-07	3.67E-08	3.07E-08	1.20E-07
Thrust Per Engine (N)	5	0.236	2.3	1.1	0.092	1.2
Number of engines	1	18	2	1	10	3
ISP (s)	3800	3250	1420	2600	3100	2912
Flow rate (kg/s)	.0129	1.04E-04	1.71E-04	4.31E-05	3.03E-05	1.18E-04
Total Propellant (kg)	5.48E+02	5.21E+03	7.89E+03	8.32E+03	6.98E+03	6.98E+03
Total TOF (s)	4.24E+04	4.99E+07	4.61E+07	1.93E+08	2.31E+08	5.89E+07
Power per engine (kW)	200	.500 - 7	5.0 - 50	0.5 - 20	.50 - 2.3	5.0 - 20
Max Power (kW)	200	7	50	20	2.3	20
Specific Mass (kg/kW)	1.1	1.1	1.3	1.1	1.1	1.3
Mass (kg)	220	7.7	65	22	2.53	26

Figure 6.1: Performance Values of Electric Propulsion Systems (11,12,23,25,27)

The VASIMR engine was noted for its ability to generate a high thrust compared to the other engines. Its spec sheet listed a thrust of 5 newtons per engine while still exhibiting a maximum specific impulse of 3800 seconds. However, these specs required a nonexistent space-rated nuclear power source. Furthermore, each engine requires 200 kW. This was deemed impractical for the initial tug setup since 200 kW is the minimum power creation requirement for the solar panels. Upon expanding to 500 kW, this engine could be considered; however, creating batteries that could sustain these engines would push the design out of the desired simplicity and low system mass. After this exercise, NASA's NEXT ion engine was considered. Its low mass and power made it worth considering further. However, after further analysis, it was found that 18 engines would only draw 90 kW. Adding the battery power draw and an assumed draw from the tug's electronics based on a value found from the ISS, the tug would only draw about 155 kW. This leaves copious room for more batteries and engines. It was deemed impractical to utilize upwards of 20 engines on the tug because of the large size relative to each module. Since simplicity is a key requirement, accounting for the avionics and plumbing for 20 propulsion systems became unmanageable. As a result, we chose an engine closer to our energy requirements. During this search, the NASA 457M-V2 50 kW Hall thruster was compared to the 300MS 20 kW Hall thruster. Both demonstrated similar values depending on how much power given to the engine. The 457M provides a higher throttle range with power ranging from 5 to 50 kW and a maximum thrust of 2.3 N. Conversely, the 300MS hall thruster exhibits a maximum thrust of 1.2 N and a power draw ranging from 5 to 20 kW. Both illustrate high specific impulses peaking at about 2800 N. Since the spacecraft will have 200 kW (later 500 kW) of available power, the 457M was chosen because it is better equipped to take full advantage of all the available power.

Hall thruster replacement was introduced into SMo-FlaKE's design due to considerations for deep space missions. With all four modules, it takes approximately 322 days to complete the trip to the Moon and return to Earth. Hall thrusters operate for about 3 years before requiring replacement (12). Therefore, any missions requiring a longer timeline will need to launch with extra engines and complete and engine replacement mid-mission. So, for a mission to Mars, it takes about three years for a one-way trip with the current configuration. Therefore, Ermine will be utilized to replace the thrusters as detailed in Section 13.

This reasoning led to exploring the challenge of replacing the hall thruster in orbit with the Yeti and/or Ermine. Yeti must place the small fine arm on a grapple fixture located near the hall thruster in need of replacing. Ermine accesses the connections through an exterior panel and begins disconnecting all the electrical connections. The precision required for this operation may require teleoperation which

would be challenging considering the distance. However, clever use of wire sleeving and signals will allow autonomous

Properties	Initial	Final
NASA-457M V2	2 Modules	4 Modules
Acceleration	3.07E-07	3.67E-08
Thrust Per Engine (N)	2.3	2.3
Number of engines	4	8
TOF escape(s) - Constant Tangent Acceleration	2.27E+07	2.13E+08
Flow rate (kg/s)	3.42E-04	6.84E+-04
Total Propellant (kg)	9.54E+03	1.58E+04
Total TOF (s)	2.79E+07	2.31E+07
Power per engine (kW)	5.0-50	5.0-50

Figure 6.2: Initial and Final 457 Specifications (25)

SECTION 7: Thermal Analysis

To get an upper estimate of the total amount of heat that needs to be dissipated, we can assume that the total amount of energy coming into the spacecraft is 200 kW in the original configuration and 500 kW in the final configuration. We can then assume that, of this total energy, any energy that does not exit the system as the kinetic energy of the exhaust becomes heat energy and must be dissipated.

Figure 7.1. Radiator Configuration

Using the specifications from the NASA-457MV2 Hall Thruster engines we calculated a total jet power of 123.5 kW from all 4 engines for the 200 kW configuration. Subtracting this value from the 200 kW produced by the solar panels we arrived at a heat generation of 76.5 kW. We calculated a total jet power of 247.1 kW from all 8 engines for the 500 kW configuration. Subtracting this value from the 500 kW produced by the solar panels we arrived at a heat generation of 252.9 kW. This includes all heat generated by non-engine avionics.

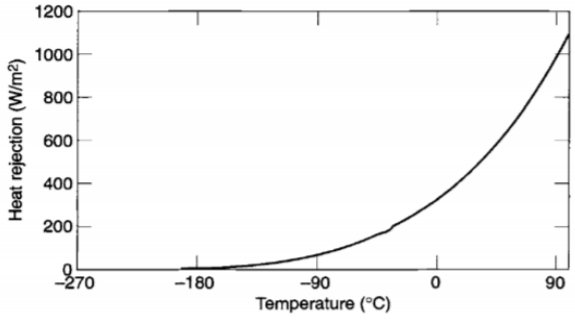

Figure 7.2: Heat rejection vs Temperature (18)

We modeled our radiator system after that on the ISS. The working fluid for our thermal control system will be ammonia “for its high thermal capacity and wide range of operating temperatures” (2). We decided not to use internal water piping and external ammonia piping and opted for complete ammonia piping because there will be no humans living in the modules that would come into contact with any leaking ammonia. Each outer module will contain its own ammonia tank, and the center module will contain a nitrogen tank and an accumulator. The nitrogen gas and accumulator work to keep the ammonia in a liquid phase and compensate for any expansions or contractions of the ammonia due to temperature fluctuations. Once all of the modules are berthed and the fluid lines are connected the ammonia will be able to circulate across all of the modules. The heat transfer

to **t**he fluids will be done within coldplates that electronic systems will sit on. The piping will bring the heated ammonia to radiators that will radiate the heat into space using radiator panels with internal ammonia piping. Once the heat is radiated from the ammonia, the fluid is routed back around into the coldplates to restart the process. We calculated the temperature at our spacecraft in orbit around the Earth to be about 256 K. Using the graph found in Figure 7.2, we found that we would ideally be rejecting heat at a capacity of 350 W/m^2.

For the 200 kW configuration, we will need 218.6 m^2 of radiator paneling. We decided to create 4 radiators comprised of 8 panels each with panel dimensions of 3.4 x 2 m giving each radiator total dimensions of 3.4 x 16.1 m. For the 500 kW configuration, we will need 722.6 m^2 of radiator paneling. We decided to reuse the radiators from the 200 kW configuration and add 8 additional radiators comprised of 8 panels each with panel dimensions of 3.4 x 2.3 m giving each additional radiator total dimensions of 3.4 x 18.6 m. The radiators will be mounted perpendicular to the solar panels to minimize the incident sunlight on the radiator panel surfaces. The radiator panels will face deep space so that no heat is radiated to the solar panels or the spacecraft.

The technology used for the berthing of the radiators is the same as the one used for the connection of the solar panels. However, there will be fluid channels that will allow the cooling fluid to flow from and back to the entire spacecraft.

SECTION 8: Structural Analysis

The outer and center modules are an octagonal shape with a radius of 2 m, a length of 8 m, and a shell thickness of 10 mm. The large size of the structure is required in order to house Yeti, propellants, plumbing, solar arrays, and the significant number of batteries. By referencing the Falcon 9 payload user's guide (8), rough estimates for launch loads on payloads ranging from 1,000 to 10,886 kg were found to peak at approximately 6 g's. Applying the aluminum 6061 material to a module, the approximate weight of each module was calculated to be 3,200 kg. Assuming a fixed constraint setup for packing the payload in the Falcon 9 and a 6 g acceleration loading on the rest of the body, the stresses and deformations were calculated in NX11. The previous figures illustrate the stresses on each module during launch. Figure 8.3 depicts the first mode to be 6.8 Hz at a load of .4 g's.

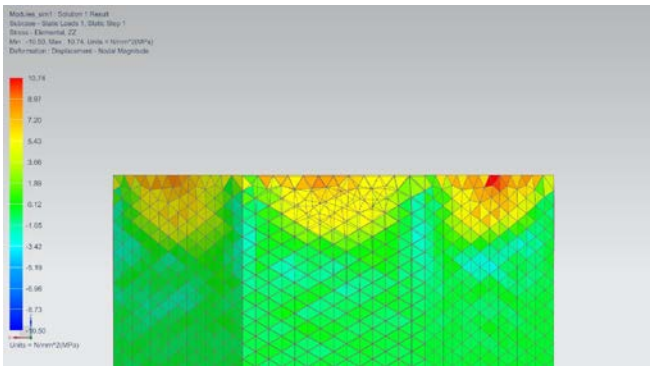

Figure 8.1 ZZ Stress

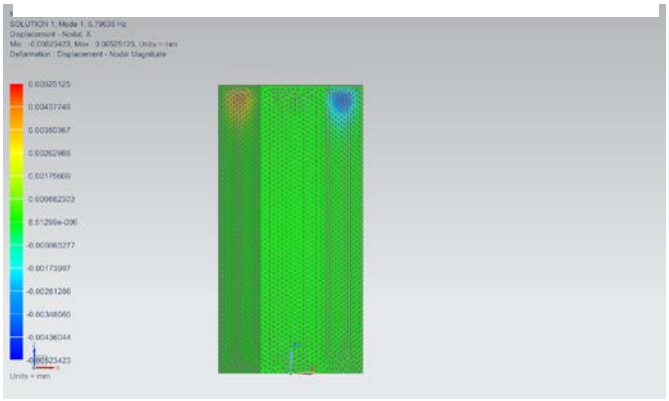

Figure 8.2 1st Node

SECTION 9: Reaction Control System

The choice of the Reaction Control System was driven by three metrics: minimizing coupling and duty cycle, and minimizing the usage of propellant. We looked at various options from the Attitude Control Motor (AMC) of Orbital to the Draco Thrusters from SpaceX. However, only the 200 N Bipropellant Thruster from Airbus and the R-40 3870 N Bipropellant Rocket from Aerojet were the two choices that offer a deal of decoupling, with thrusting providing 5 degrees of freedom for each module. We then did a comparison study between those two options. We simplify our spacecraft as a cylinder of radius (moment arm from the thrusters to the center of mass). Using the parallel axis theorem, Euler's second law, we were able to derive the metrics in the table below. We determine the propellant use by multiplying the firing timing by the mass flow rate.

Figure 9.2 shows the profile of the propellant mass as the swept angle increases. The 200 N Bipropellant uses less propellant to execute the same maneuver. To compare the respective duty cycle, we assume a dead band of 5 degrees. It can be determined from Figure 9.1 that the 200N Bipropellant Thruster as a smaller duty cycle, which means it is optimal for position keeping. Based on this analysis, we concluded that the 200N Bipropellant Thruster was the optimal RCS for our design due to its lighter mass without compromising thrust. Lastly, it's the only space qualified RCS from our trade study.

REACTION CONTROL SYSTEM (RCS)	Fuel and Oxidizer	Mass (kg)	Thrust (N)	Status	Manufacturer
Apollo RCS quadrant	MMH and NO4	43.2 kg	450	Successfully flown	Grumman Aerospace Corporation
Draco Thrusters	MMH and NO4	Not available	400	Successfully flown	Space X
R-40 3870N Bipropellant Rocket	MMH/NTO(MON-3)	6.8 kg	111	Successfully flown	Aerojet
200 N Bipropellant Thruster	MMH and MO-3	9.5 kg	236	Space qualified	Airbus

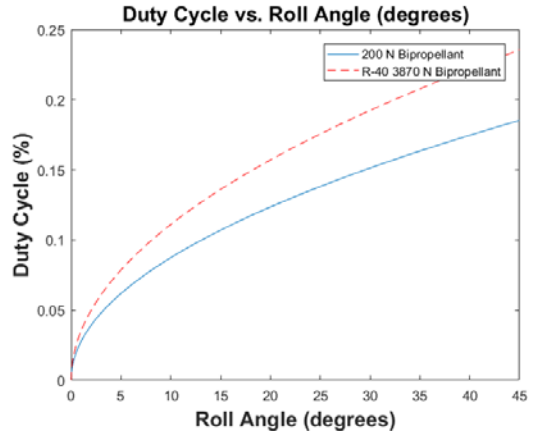

Figure 9.1 Duty Cycle vs. Roll Angle

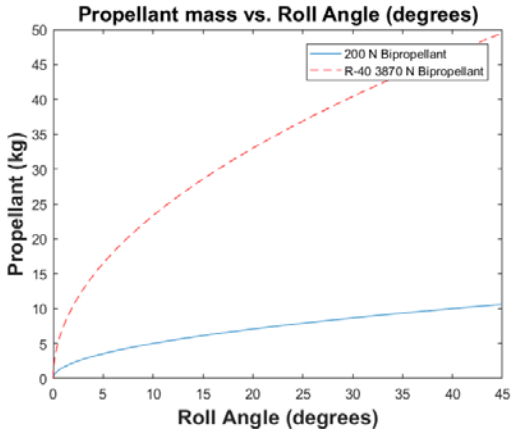

Figure 9.2 Propellant mass vs. Roll Angle

SECTION 10: Fluid Distribution System

The four main fluids running throughout our spacecraft will be the Xenon for the Hall thrusters, fuel and oxidizer for the RCS system, and ammonia for the radiators. Each of the outer modules will contain tanks that will hold enough of each fluid for the module to last through its designed lifetime. However, in the case of a module failure, engine failure, or any other unforeseen problem, the center module features a pump system and two holding tanks that allows for fluid transfer between modules and storage space for additional fluids if required. In figure 10.1 on the right, three different ideas are shown for how the center module pump system could work.

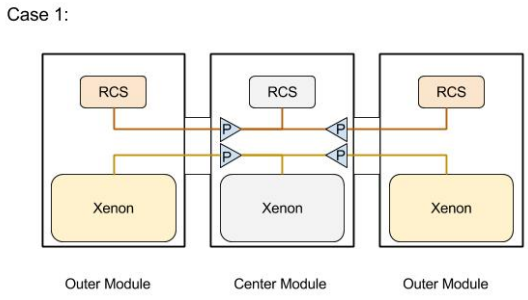

Figure 10.1 Case 1: Two Tanks

All three cases rely on a pump and valves to control the flow of xenon. The pump will use the valves

to control which module the xenon flows to and if the xenon goes into the holding tank. Case 1 shows two separate holding tanks, one for the RCS propellant and one for xenon. However, due to space restrictions, we did not choose this case. Case 2 shows one solid holding tank with 2 separate bladders within the tank, one for each fluid. This case was chosen as it allowed for either propellant or RCS to be stored, or both and not have to worry about wasted space. Case 3 shows that the RCS propellant is pumped directly from one outer module to another, however in the case of excess RCS propellant there would be nowhere for it to be stored so this case was not chosen. The holding tank in the center module only holds extra RCS propellant and Xenon as both of these propellants will be lost over the lifetime of the spacecraft unlike the Ammonia, which circulates throughout the radiator system. Some issues that can occur within this system are broken or leaking pipes. This can be addressed by using the small fine arm to change pipes, or add sleeves over broken sections of pipe. Another major issue, is the case of the center tank or bladders breaking, this cannot be fixed in space and would need to be replaced. If the center tank is broken, the fluid can bypass the tank and be transferred directly from one module to another.

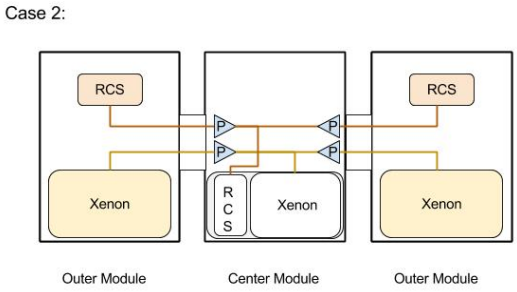

Figure 10.2 Case 2: 1 Tank and 2 Bladders

C:

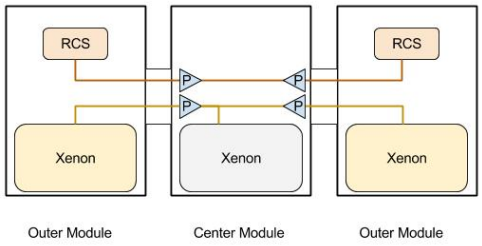

Figure 10.3 Case 3: 1 Tank

SECTION 11: Mass Breakdown

The detailed mass breakdown is listed in Figure 11.1. The solar arrays that we chose had a mass of 1.76 kg/m^2. The values tabulated above come from surface areas of 576 m^2 and 1,416 m^2 for the original and expanded configurations. The mass of the solar array support structure and gimbals was estimated to be about 10% of the mass of the solar arrays. Each Hall Effect Thruster weighs 136 kg and has its own titanium propellant tank. Each propellant tank weighs 88 kg and carries about 1,760 kg of Xenon gas, stored at 8.3 MPa. The mass of the propellant tanks is based on the ideal storage pressure and density of xenon: the ideal density is about 1.35 g/ml or about 1350 kg/m^3 (7). To design the tanks for their maximum possible pressure, we must calculate the pressure in LEO, which is when the tanks are full and the ambient temperature is greatest (about 300 K). With these assumptions, the tanks were designed to withstand a pressure of 8.3 MPa with a safety factor of 1.1 (NASA standard for propellant tanks). Each engine also has 9 batteries, which each weigh 13 kg, and the central payload-bearing module has 2 batteries, for a total of 38 batteries. There are 2 RCS systems, 5 thrusters per system. Each thruster with all the required wiring, avionics, and structural support weighs 1.9 kg. The mass of the engine gimbals was found to be 184 kg.

Item:	Mass initial (kg):	Mass final (kg):
Solar Panels:	1,014	2,492
Batteries:	1,534	2,990
SEP Engines:	544	1,360
Propellant	1,760	1,760
Prop. Tank Mass:	880	880
RCS Thrusters:	19	19
RCS Propellant:	900	900
Solar Array Joints:	1,152	2,304
Wiring:	361	473
Shell Structure:	9,600	16,000
Truss Connectors:	2,802	3,736
Thruster Gimbals:	185	462
DDU:	78	194
Radiator:	4,146	12,078
Robot Arm:	1,800	1,800
Payload	10,000	15,000
Alpha Joints:	1,152	2,304
Grapple Fixtures:	1,656	2,760
Ermine:	587	587
Passive CBM:	789	1,315
Active CBM:	566	943
Total	41,523	73,898

Figure 11.1 Mass Breakdown Table

SECTION 12: TRL Critical Items

The technologies that have a technology readiness level (TRL) of less than six are the direct-drive unit (DDU) and the NASA-457Mv2. The DDU has a TRL level of 2-3, but this is only speculation as each DDU is custom built to the mission it is needed for however, no mission as of yet has used the size engines that we are using. The NASA-457Mv2 50 kW Hall Effect

Thrusters have a TRL level of 4-5 since the system model has been tested in the laboratory environment and shown to work (24). All other technology used on the spacecraft has a TRL level of six or higher. Lastly, the Yeti and Ermine are both experimental, so they will have TRL levels of 4 by launch.

SECTION 13: Robotic Assembly

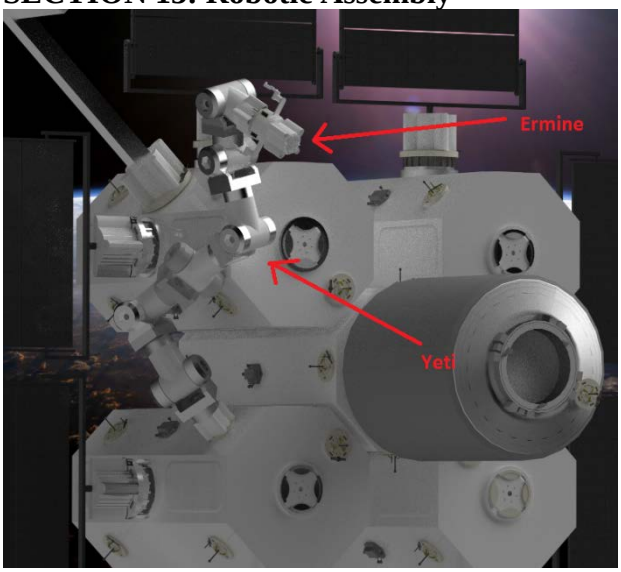

Figure 13.1 Yeti and Ermine Together

The robotic arm design consideration derived mainly from needing high maneuverability to navigate the spacecraft while retaining the appropriate amount of strength to berth modules and replacement parts. As a result, the Canadarm2 was initially considered as inspiration for the arm since it utilizes an inchworm motion to traverse the ISS.Therefore, a six degree of freedom arm consisting of a series roll and pitch joints was proposed. Its serpent-like structure offers agile movement as it inchworms across modules and slides past the gaps between solar panels and radiators. Additionally, the arm has access to a small fine arm named Ermine. This end effector emulates the processes of DEXTRE onboard the ISS. On SMo-FlaKE, it's mainly utilized to perform more dexterous tasks like disconnecting electrical connections or replacing interior plumbing with its drill and hand end effectors. Additional end effectors can be added to improve Ermine's abilities and overall. The interface for inchworming across the spacecraft employs the replaceable Power and Data Grapple Fixture. These are located around several key points on SMo-FlaKE. For example, grapple fixtures are located near the common berthing mechanism, solar panels and exterior panels to close the distance between Ermine and its task. Yeti attaches to these grapple fixtures through an end effector similar to Canadarm2 in order to take advantage of the proven capture before contact technology. On launch, the arm measures about 6 meters so it can reach most grapple fixtures once it deploys from the center module.

When assembling the tug, the center module is launched into LEO with 2 batteries, full xenon and RCS tanks, Yeti and Ermine. Afterward, an outer module is launched containing batteries, full fuel tanks, two solar panel capsules and one radiator. To berth the outer module with the center, the rcs and hall thrusters maintain a steady orientation for Yeti to successfully operate. After the outer module is jettisoned from its payload fairing, it can autonomously navigate to the desired location for docking utilizing its hall and RCS thrusters. Yeti will receive a signal from the TriDar sensors on the center module when the outer module is within 30 meters. This begins the autonomous berthing process. To calculate the total assembly time, the speed of operations for Canadarm2 can be used after considering the lower technology readiness level of Yeti and its smaller size. Combining this with the dimensions of SMo-FLaKE's modules allows rough assembly times to be calculated. Using the speed of operations of the Candarm2 (6) and dividing them by 80 to provide ample space for the lower TRL, it takes Yeti 5.5 days to assemble both outer modules. Additionally, Yeti requires 6.7 hours to traverse the entire craft. The entire initial configuration of SMo-FLaKE requires one center module, two outer modules, four solar panels and two radiators. Assuming Yeti grabs all the components when they are six meters away, it takes a total of 734400 seconds or about 8.5 days. Also, cooldown time for bolting the common berthing (13) mechanism is about 24 hours between the two modules brings the total assembly time to 34 hours. This time calculation assumes Yeti starts from the center, moves to the outer edge of the center module, berths the first outer module, attaches three capsules, moves across to the center module edge, assembles the other outer module and its capsules and returns to the center. Yeti will inchworm to the grapple fixtures

located on edge closest to the center module. Then, it straightens out to 6 meters and awaits another signal from the distance sensors at the tip of Yeti. Once the center module is within 20 meters, the Yeti takes advantage of the capture before contact technology available in the Canadarm2 end effectors and accompanying grapple fixtures to begin berthing procedures. The autonomous berthing process involves a communication process between the center and outer module's onboard inertial navigation units and distance sensors to calculate the center and outer modules positions. This data feeds into the Yeti's control scheme which allows it to attach to the power and data grapple fixtures located on the outer modules. Lastly, Yeti can orientate the outer module to ensure it successfully merges with the CBM's fluid and power transfer modifications. Once both modules are berthed, the center module receives a signal from the outer module through the berthing mechanism that the process is complete. Yeti begins removing the solar panel and radiator capsules by grabbing the latchable grapple fixture located on the capsule. Yeti orientates the capsule until its end effector is aligned to the appropriate grapple fixture located on the outer module and then berths. Afterward, the capsule is jettisoned off the solar panel and a signal is sent through the grapple fixture to the assembly driver motors and deployment begins. The same process is repeated for each module, solar panel and radiator needed.

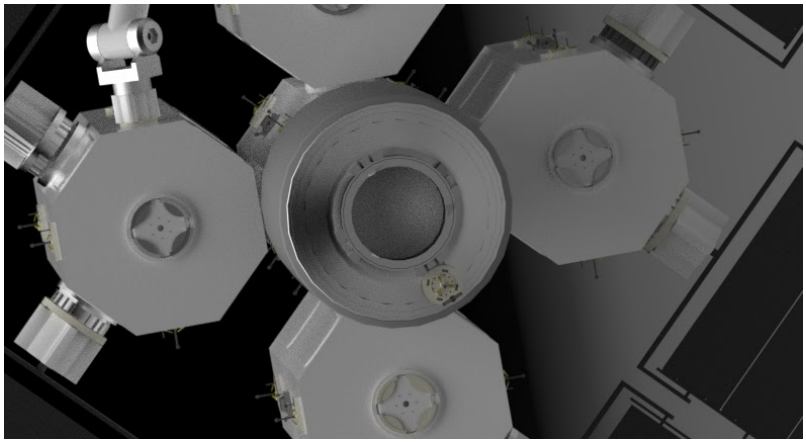

Figure13.2 Payload Configuration

Any SMo-FlaKE payloads will be launched into LEO with passive CBM rings to attach to any of the active CBM rings on the outer modules. These CBM connections will be the same mechanism as the CBM rings used for berthing the outer modules to the center module. Since there will be fluid and power connections, the payload ports can be used to refuel or recharge the payload or SMo-FlaKE modules. Similarly, for autonomous payload berthing, the Yeti receives an alert signal when the payload is within 30 meters. Then, it initiates the berthing process by inchworming to any of the grapple fixtures located near the payload. Yeti will attach one end effector to this latchable grapple fixture and lock the other end effector to the flight-releasable grapple fixture located on the outer end of the payload. Then, the payload is pulled into the berthing mechanism and provided power if needed. However, depending on the size of the payload and robustness of the control code for the arm, teleoperation may be required to successfully berth the payload. Additionally, any cargo not initially stored within the modules will be brought up with the payload and stored within the payload or, using the arm, moved from the payload to the modules. All future modules and components require the same grapple fixture, end effector and CBM as described above.

Repairing the Yeti requires any damaged links to be replaced. This can be autonomously completed by initiating a replacement protocol. Yeti will seek out the closest grapple fixture and lock in place. Then, Yeti will replace all defective links with replacements located inside of a module. The small fine arm and any future end effectors can reside in this area. If both end links become inoperable, the arm enters a critical state and must be replaced. The modular nature of the arm allows it to continue temporarily function with the loss of links. Additionally, the choice of power data grapple fixtures ensure compatibility with the Canadarm2 and its end effectors. If enough grapple fixtures became inoperable, the arm could not traverse the vehicle properly and would require entire module replacement. The ability for this particular grapple fixture (12) to be replaced and moved in orbit allow for vast customization of modules and component placement for the future and prevents spacecraft loss due to faulty grapple fixtures.

Piezoelectric sensors on the hull of SMo-FlaKE will process information on Micrometeoroid and Orbital Debris (MMOD) impacts and locate where the impact occurred. This system would be designed after the Distributed Impact Detection System (DIDS) (28). If one or two sensors were to stop working then the system should still be able to extrapolate if there was an impact on a broken sensor by the readings gathered from the surrounding sensors. There is the concern that an impact on a broken sensor may not break the alarm threshold on the surrounding sensors to notify the system that there was an impact. For this reason the sensors should be replaced as soon as possible for system integrity. As soon as the DIDS detects an impact Yeti will move to the location and send camera feed to mission control. Then, Mission control will analyze the damage and decide on with action to pursue depending on the damage from the impact. These actions include: repairing the affected area with welding, replacing the entire module, or doing nothing because the damage is negligible.

SECTION 14: Launching Configuration

The launching configuration of SMo-FlaKE will consist of three launches on the Atlas V 511 rocket. The payload capacity of the Atlas V 511 for a LEO orbit is 11,000 kg (25). Using the mass estimations table, we calculated that each of the outer modules will have a mass of approximately 8,700 kg and the inner module will have a mass of approximately 6,200 kg. The Atlas V payload fairings allow for a payload size of diameter 5 meters and height 11 meters. The payload fairing has a total height of 16 meters, however after 11 meters the fairing starts to converge to a cone. Our modules have a diameter of 4 meters and a height of 8 meters, therefore they will fit within the payload fairings of the Atlas V. On each launch, the payload will have one module, with a radiator stacked on top.

Additional launches for replacement parts can use a range of launch vehicles, with the largest vehicle being the Atlas V 511 which would carry a replacement module. All replacement parts will be flown to SMo-FLaKE where they will be connected to the one of the spacecraft's CBMs. Once connected, the replacement parts will be taken off the payload and attached using Yeti and Ermine. The old parts will be placed on the payload which will then be flown back into Earth's atmosphere to be destroyed, reducing waste in space.

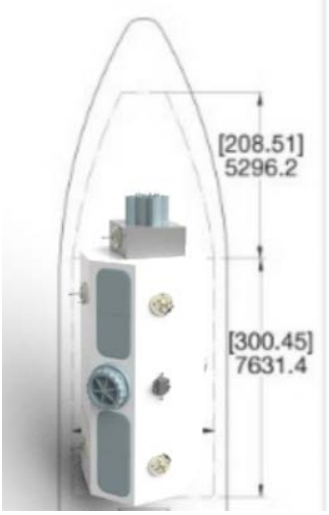

Figure 14.1 Launch Configuration

SECTION 15: Ground Testing

Before launch, a number of spacecraft components must be tested on the ground. We must verify: the structural integrity of shell structure, joints, propellant tanks, gimbals, solar arrays, radiators and their support structures under both acceleration and thermal loads, the thrust profile and other engine properties in microgravity, and the ability of Yeti to assemble modules in low-gravity.

The structural integrity of the various spacecraft components can be tested in NASA's high bay, either at JSC or JPL. Testing of the Hall Thruster in low-gravity and low-pressure situations is a bit more difficult. Testing in parabolic flight is not an option because of the severe time constraints. Using a Neutral Buoyancy Facility is not an option, because the thruster would have to be designed to be waterproof and the pressure at depth is far greater than what the thruster can expect to experience in space. This testing requires highly specialized facilities, located at high altitudes with the proper vacuum chambers. Fortunately, these specialized facilities already exist and are being used to test Hall Thrusters. We can test fire the thrusters at these facilities on the ground before launch.

To test the capabilities and functionality of Yeti, we propose the use of the Neutral Buoyancy Research Facility that is part of the Space Systems Laboratory at the University of Maryland, College Park. With dimensions of 25 x 50 ft, the NBRF at SSL is large enough to test the assembly of our modules. This will require that we manufacture Yeti such that it is neutrally buoyant and can be operated

at underwater pressures, but we will still be able to guarantee that Yeti has the dexterity required to assemble the modules in zero-gravity.

SECTION 16: Project Planning

Mission Statement				
	MS1		Teams will design and analyze potential concepts and systems to provide the ability to achieve a 200kW SEP tug for transferring payloads between LEO to LDRO and LDRO and LEO.	
Requirements				
M			**Mission Requirements**	**Source**
	M-1		The spacecraft shall self assemble in space within 60 days	MS1
	M-2		The spacecraft shall be propelled by electric propulsion	MS1
	M-3		The spacecraft shall produce 200kW at the beginning of life	MS1
	M-4		The spacecraft shall derive all power from solar arrays	MS1
	M-5		The spacecraft shall transfer payloads from LEO to LDRO	MS1
	M-6		The spacecraft shall have modular joints and arrays that can react up to 0.4 g's of acceleration	MS1
	M-7		The spacecraft shall expandable to a 500kW SEP tug for Deep Space missions	MS1
	M-8		The spacecraft shall have a fundamental flexible body vibration mode of 0.05 Hz or higher	MS1
S			**System Requirements**	**Source**
	S-1		The spacecraft shall be modular	M-1
	S-2		The spacecraft shall be launched in separate pieces	M-1
	S-3		The spacecraft modules shall be compatible with the robotic assembly mechanism	M-2,M-4,M-5
	S-4		The spacecraft shall be flight certified for long mission in deep space	M-6
	S-5		The spacecraft shall be reusable, repairable and upgradable by replacing modules	M-6
	S-6		The spacecraft shall provide enough thrust to travel: LEO -> Moon's orbit around Earth -> LDRO	M-4
	S-7		The spacecraft shall be mass efficient (light weight)	M-2
	S-8		The spacecraft shall be required the fewest number of launch	M-1
S1			**Propulsion System Requirements**	**Source**
	S1-1		The propulsion system shall have room to accomodate additional engines upon the addition of new solar arrays	S-5
	S1-2		The propulsion system shall provide enough deltaV = deltaVLeo - deltaVmoon + deltaVLDRO	S-8
	S1-3		The propulsion system must be powered by electricity	M-2
	S1-4		The propulsion system shall have a T/W ratio such that adding more solar arrays and more engines improves performance	M-7
	S1-5		The propulsion system shall include all thrusters required for in-orbit manuevers	
S2			**Power System Requirements**	**Source**
	S2-1		The power system joints shall withstand a load of up to 0.4 g's of accelerations	M-5
	S2-2		The power system shall contain all robotic assembly mechanisms	S-3
	S2-3		The power system shall be able to transfer up to 500kW of power to other systems	M-6,S-4
S3			**Modular launching, Order of Launches Requirements**	**Source**
	S3-1		The power system shall launch first	S-1
	S3-2		The propulsion system shall launch second	S-1

Figure 16.1 Requirements Verification Matrix

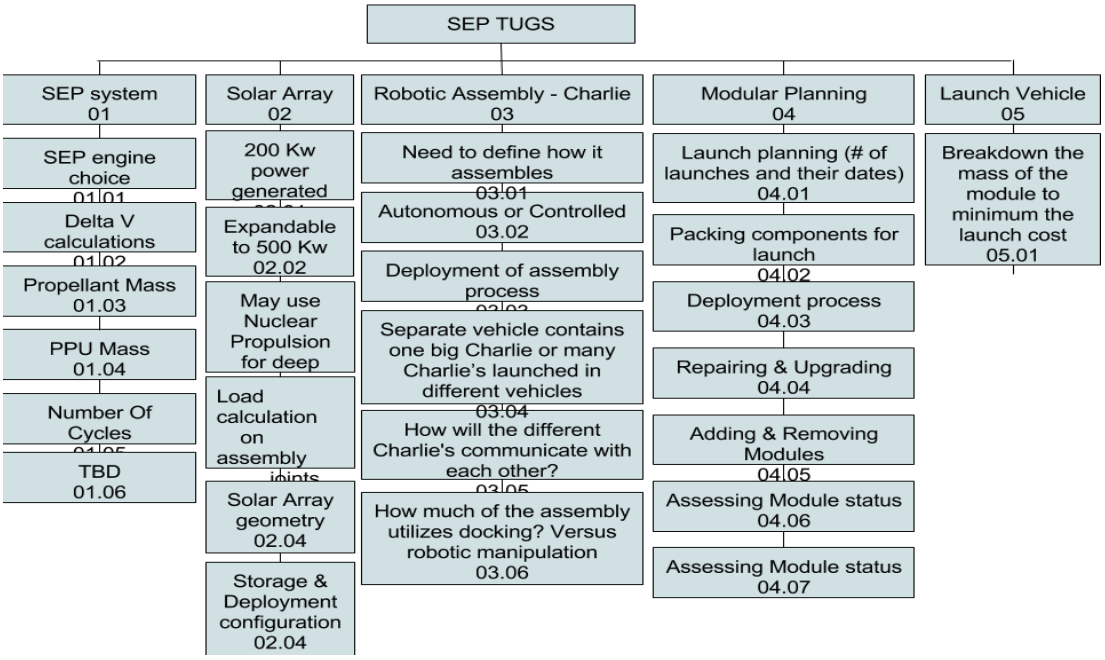

Figure 16.2 Work Breakdown Structure

References:

1. Airbus Safran Launchers. “200 N Bipropellant Thruster.” (2003). Web. 29 Jan. 2017. <http://www.space-propulsion.com/spacecraft-propulsion/bipropellant-thrusters/220n-atv-thrusters.html>
2. Boeing. *Active Thermal Control System (ATCS) Overview*. N.p.: NASA, n.d. PDF. <https://www.nasa.gov/pdf/473486main_iss_atcs_overview.pdf>.
3. Brophy, John R., M. Andy Etters, Jason Gates, Charles E. Garner, Marlin Klatte, C. John Lo, Michael G. Marcucci, Steve Mikes, Masashi Mizukami, Barry Nakazono, and Greg Pixler. Proc. of International Electric Propulsion Conference, Italy, Florence. N.p., n.d. Web. 15 Nov. 2016. <http://erps.spacegrant.org/uploads/images/images/iepc_articledownload_1988-2007/2007index/IEPC-2007-083.pdf>.
4. Buchmann, Isidor. "How Does Internal Resistance Affect Performance?" *Basic to Advanced Battery Information from Battery University*. N.p., 2016. Web. 15 Nov. 2016. <http://batteryuniversity.com/learn/archive/how_does_internal_resistance_affect_performance>.
5. Callen, P. (2014, June). Robotic Systems. In *Robotic Transfer and Interfaces for External ISS Payloads*. Retrieved from <https://ntrs.nasa.gov/archive/nasa/casi.ntrs.nasa.gov/20140008717.pdf>
6. *Dunbar, B. (2013, January 08). Canadarm2 and the Mobile Servicing System. Retrieved from* <https://www.nasa.gov/mission_pages/station/structure/elements/mss.html>
7. Evans, G., and S. Gordon. "Propellant Storage Considerations for Electric Propulsion." 8th Joint Propulsion Specialist Conference (1972): n. pag. Spacegrant.org. Web. http://erps.spacegrant.org/uploads/images/images/iepc_articledownload_1988-2007/1991index/IEPC1991-107.pdf
8. Falcon 9 Users Guide rev02 - SpaceX. (2015, October 21). Retrieved November 17, 2016, from http://www.spacex.com/sites/spacex/files/falcon_9_users_guide_rev_2.0.pdf
9. Howard, R. T., Bryan, T. C., Brewster, L. L., & Lee, J. E. (2009). Proximity Operations and Docking Sensor Development. Retrieved February 6, 2017, from https://ntrs.nasa.gov/archive/nasa/casi.ntrs.nasa.gov/20090025872.pdf
10. Kamhawi, Hani, and Wensheng Huang. "Performance and Thermal Characterization of the NASA- 300MS 20 KW Hall Effect Thruster." *Performance and Thermal Characterization of the NASA-* (n.d.): n. pag. NASA, 6 Oct. 2013. Web
11. Kamhawi, H., Hang, T., Smith, T., Herman, D., Huang, W., & Shastry, R. (n.d.). Performance Characterization of the Air Force ... Retrieved February 6, 2017, from https://ntrs.nasa.gov/archive/nasa/casi.ntrs.nasa.gov/20140010771.pdf
12. Manzella, D. (2007). Low Cost Electric Propulsion for Deep Space Robotic Missions. Retrieved February 6, 2017, from https://esto.nasa.gov/conferences/nstc2007/papers/Manzella_David_D10P2_NSTC-07-0116.pdf
13. McLaughlin, Richard J., and William H. Warr. “The Common Berthing Mechanism (CBM) for International
Space Station.” (2001). Honeywell Engines and Systems. Web. 29 Jan. 2017. <http://spacecraft.ssl.umd.edu/design_lib/ICES01-2435.ISS_CBM.pdf>
14. Merrill, Raymond Gabriel, Thomas Kerslake, John R. Brophy, Robert Gershman, Nathan Strange, and Damon Landau. "300-kW Solar Electric Propulsion System Configuration for Human Exploration of Near-Earth Asteroids." (n.d.): n. pag. Bigidea.nianet.org. NASA, 2011. Web. 13 Nov. 2016. <http://bigidea.nianet.org/wp-content/uploads/2016/10/300-kW-Solar-Electric-Propulsion-21.pdf>.
15. Orbital ATK. "Ultraflex Solar Array Systems." *Orbital ATK*. Orbital ATK, 2015. Web. 5 Nov. 2016.
16. Parker Snap-tite. “28-1 Series.” (2015). Web. 15 Jan 2017. <http://www.snap-titequickdisconnects.com/products/drybreak_non-spill_couplings/28-1_series/index.html>
17. Pinero L., Peterson P., and Bowers G. "High Performance Power Module for Hall Effect Thrusters." *High Performance Power Module for Hall Effect Thrusters* (n.d.): n. pag. *NASA*. NASA, Sept. 2002. Web. 6 Nov. 2016. <https://ntrs.nasa.gov/archive/nasa/casi.ntrs.nasa.gov/20030003703.pdf>.
18. Rochus, P., and L. Salvador. “Spacecraft thermal control.” November 2011. <http://www.ltas-vis.ulg.ac.be/cmsms/uploads/File/SC_Thermal_Control_Satellite_Engineering_28Nov2011.pdf>
19. Ruel, S. (2010). TriDAR Model Based Tracking Vision System for On-Orbit Servicing. Retrieved February 6, 2017, from

https://sspd.gsfc.nasa.gov/workshop_2010/day3/Stephane_Ruel/OOS_Workshop_TriDAR_Presentation.pdf
20. Saft. "Battery Search." *Battery Search | Saft*. N.p., 2016. Web. 5 Nov. 2016. <http://www.saftbatteries.com/solutions/products/battery-search>.
21. Saft. *Saft-SpaceBrochure*. Paris: Saft, 2016. Feb. 2016. Web. 5 Nov. 2016. <http://www.saftbatteries.com/force_download/1602_Saft-SpaceBrochure_8.5x11_1.pdf>
22. Schmidt, G. R., Patterson, M. J., & Benson, S. W. (2008). The NASA Evolutionary Xenon Thruster (NEXT): The Next Step For U.S. Deep Space Propulsion. Retrieved February 6, 2017, from https://ntrs.nasa.gov/archive/nasa/casi.ntrs.nasa.gov/20080047732.pdf
23. Spectrolab Inc. "Space Solar Panels." (n.d.): n. pag. *Spectrolab.com*. Spectrolab, 2015. Web. 5 Nov. 2016. <http://www.spectrolab.com/DataSheets/Panel/panels.pdf>.
24. Soulas, George, Thomas Haag, Daniel Herman, Wensheng Huang, Hani Kamhawi, and Rohit Shastry. "Performance Test Results of the NASA-457M V2 Hall Thruster." *48th AIAA/ASME/SAE/ASEE Joint Propulsion Conference & Exhibit* (2012): n. pag. NASA, 1 Aug. 2012. Web.
25. ULA. "Atlas V." *Atlas V - United Launch Alliance*. United Launch Alliance, 2015. Web. 01 Dec. 2016. <http://www.ulalaunch.com/Products_AtlasV.aspx>.
26. Variable Specific Impulse Magnetoplasma Rocket. (n.d.). Retrieved February 06, 2017, from https://en.wikipedia.org/wiki/Variable_Specific_Impulse_Magnetoplasma_Rocket
27. Walcer, Mike. (2004). Distributed Impact Detection System [Technical Abstract]. *Inspection and Diagnostics*. Web. 29 Jan. 2017. <http://sbir.nasa.gov/SBIR/abstracts/04/sbir/phase1/SBIR-04-1-X4.03-8276.html>